

**FINITE ELEMENT MODELLING OF ULTRASOUND
PROPAGATION IN LONG BONES DURING FRACTURE
HEALLING**

**I.C. Kourtis, V.C. Protopappas, L.C. Kourtis, D.I. Fotiadis
and C.V. Massalas**

05– 2003

Preprint, no 05 – 05 / 2003

**Department of Computer Science
University of Ioannina
45110 Ioannina, Greece**

Finite Element Modelling of Ultrasound Propagation in Long Bones during Fracture Healing

I.C. Kourtis¹, V.C. Protopappas¹, L.C. Kourtis¹, D.I. Fotiadis^{1,3} and C.V. Massalas^{2,3}

Summary

In this work, the vibrational analysis and ultrasound wave propagation in long bones during fracture healing is studied using the Finite Element Method. The aim of this study is to investigate the influence of callus maturation on the vibrational behavior of the bone and ultrasound propagation. The geometrical and mechanical properties are obtained from CT scans. The callus maturation is studied as a five-stage procedure. The obtained results are compared with experiments.

Introduction

Fracture healing of long bones is a dynamic process which involves the formation and maturation of a regenerative soft tissue called callus. Nowadays, the assessment of the healing progress can be achieved by X-rays and manual sensing of the fractured bone. Those techniques are highly subjective to the surgeon's experience. Therefore, methods which can provide quantitative information on the progress of fracture healing constitute valuable diagnostic tools.

Vibrational analysis [1-7] and ultrasound measurements [8-13] have been employed to study the dynamic behavior of intact and healing long bones. Vibrational techniques include the experimental, analytical and computational determination of the modes of vibration, the resonant frequencies, the frequency response and the damping ratios. Experimentally, the vibrational behavior can be studied either using the impulse response method (with the impact of a hammer) [1,3,4] or the application of a vibration using a shaker [2]. The propagated mechanical waves are recorded by means of accelerometers or microphones. The frequency response is calculated using Fourier analysis of the response waveform divided by the impact force and the resonant frequencies are obtained. Furthermore, placing the sensors at various sites on the bone, the induced bending modes can be identified, one in the sagittal plane (displacement in the anterior-posterior direction) and one in the frontal plane (in the lateral direction). Theoretical models have also been employed to estimate the resonance frequencies. These models are based on the exact bone geometry or they are more generic to include material properties [1,6]. In addition, models using Finite Elements (FE) have been extensively employed to account for realistic geometrical characteristics and material properties and to computationally determine the vibrational modes and resonance frequencies [4-6]. The evaluation of the computational results is often achieved by comparison with experimental observations.

The fracture healing progress is assessed using vibrational analysis *in vitro* as well as *in vivo*. The resonance frequencies increase with the healing progress and this is due to the

¹ Unit of Medical Technology and Intelligent Information Systems, Dept. of Computer Science, University of Ioannina, GR 45 110 Ioannina, Greece

² Dept. of Materials Science, University of Ioannina, GR 45 110 Ioannina, Greece

³ Biomedical Research Institute - FORTH, GR 45 110 Ioannina, Greece

gradually increasing bending rigidity. However, *in vivo* measurements of the vibrational characteristics are strongly affected by the type of fracture, fixation and the damping from adjacent bones, muscles and joints. Studies on more controllable models include the use of rods connected together [1], the gradual weakening of fresh and dry long bones (by reducing the cross-sectional area [3]) and osteotomised bones filling the fracture gap with epoxy adhesive [3] or bone cement. Finite Element modeling of the healing bone is performed by incorporating a model for callus evolution to describe changes in material properties and geometry [5,15]. However, this is still very limited and restricted to simplified models.

Ultrasound techniques are used for the determination of bone mechanical properties and the monitoring of fracture healing. These techniques employ two or more ultrasound transducers operating in through-transmission mode. The propagation velocity is related to the material properties of bone and callus, whereas vibrational analysis provides with information concerning the whole bone mechanical properties (bending rigidity). *In vitro* ultrasound experiments on submerged Perspex rods in various configurations [10,11] and on osteotomised bones in a water bath [9] have been performed to investigate the ultrasound wave propagation. *In vivo* measurements on healing bones and the contralateral bone have shown an increase in propagation velocity with healing progress, but the effect of the overlying soft tissues and the limited access to the fracture region influence the repeatability and accuracy of the transcutaneous measurements [8-11]. To overcome these problems, transducers arranged in various configurations have been used to measure the skin thickness [10], with transducers being mounted on intra-osseous needles [12] or implanted in the fracture site [13].

In this work, we study the vibrational behavior and ultrasound wave propagation using Finite Element models of healing bones to assess callus maturation. 3-Dimensional (3D) FE model of sheep tibia has been reconstructed from Computed Tomography (CT) scans. The models include bone realistic geometry and material properties and the bone healing is simulated using five callus maturation stages.

Materials and Methods

A 3-Dimensional FE model of the tibia has been developed from CT scans (parameters: 120kV, 180mAs). The geometry is obtained from 3mm thick slices taken at 1.25mm intervals. Non uniform Rational B-Spline (NURBS) surfaces were constructed to represent the boundary solid model. The FE solid mesh was obtained using MSC/PATRAN software consisting of 72378 tetrahedral elements (and 15305 nodes) with a mean edge length of 2mm. An important aspect of our study is that the bone is assumed inhomogeneous in contrast with previous works [4,5]. Density values are assigned to each element from bone mineral density (BMD) measurements obtained using Quantitative CT (QCT) [14]. The bone is assumed linear elastic and isotropic. The elastic properties of bone were estimated from correlations between density (ρ) and Young's Modulus (E) [6,14]. In our study we adopted the following relationships:

$$E \propto \begin{cases} \rho^{2.5}, & \text{if } \rho < 1.2 \text{ gr/cm}^3 \\ \rho^{3.3}, & \text{if } \rho > 1.2 \text{ gr/cm}^3 \end{cases} \quad (1)$$

Therefore the assumption of bone isotropy holds only from a macroscopical point of view, since elasticity is a function of density.

Callus is placed at the mid diaphysis and its maturation is modelled as a five-stage process. Throughout these stages, callus geometry and material properties evolve as a result of the

healing process. The assigned values are given as a percentage of the mean density and Young Modulus of the cortical bone as shown in Table 1. More specifically, the first stage is described by low density (similar to water) and elasticity parameters, which correspond to the first sequence of physiological events following a fracture, where haematoma and cell proliferation take place. Later stages are characterised by gradually increasing values simulating callus development and consolidation.

Table 1: Callus material properties at each simulation stage

Maturation Stage	ρ (gr/cm ³)	E (MPa)
0.1%	1.1	11.5
1%	1.18	115.0
10%	1.28	1150.0
50%	1.45	5750.0
100%	1.80	11500.0



Figure 1: Callus geometry evolution during fracture healing.

Moreover, the geometry variation of callus as it progressively bulges out the periosteum and into the medullary canal is also taken into account at each stage (Fig. 1).

We pay attention to two cases: in the first zero stress applies on the external and internal surfaces and in the second the bone is fixed at the four pins of a unilateral external fixator which is considered to be a rigid fixed body. The muscle and the joints support are not taken into account in our study. For each case we compute the eigenfrequencies and vibration modes.

In addition, we have studied the ultrasound wave propagation through the FE bone model. Our aim is to determine how callus maturation influences the propagation velocity and the frequency response. We apply a displacement normal to the free face of the elements on a 6mm diameter area (stimulus origin). The displacement waveform follows the actual vibration of a broadband ultrasound transducer having 1MHz central frequency. The propagating wave is recorded at a 20mm distance, on the opposite side of the fracture site in the axial direction. This area is 6mm in diameter (target). Target nodal surface displacements are averaged resulting in a measure that represents the received ultrasound wave. The transition time is measured and the propagation velocity is calculated. The frequency response ($A(f)$) is determined by the spectrum of recorded ultrasound waveform divided by the spectrum of the excitation displacement:

$$A(f) = 10 \log \left(\frac{P_{rec}(f)}{P_{exc}(f)} \right) \quad (2)$$

where f is the cyclic frequency and P_{rec} and P_{exc} is the Power Spectral Density (PSD) of the received waveform and the excitation pulse, respectively.

The computational results of the ultrasound study are compared with experimental measurements performed *in vitro*. The bones are osteotomised at the mid diaphysis and stabilised with one plane external fixation. Two ultrasound transducers (Valpey Fisher, custom order) are mounted onto the bone in the same configuration as in the FE model. Three biological materials are inserted consequently in the fracture gap to simulate callus consolidation. These include muscle ($\rho=1.1 \text{ gr/cm}^3$, $E=79\text{KPa}$ under zero loading) which corresponds to the early healing stages, cartilage ($\rho=1.05 \text{ gr/cm}^3$, $E=500\text{KPa}$) which represents the formation of blocks of cartilage within callus and trabecular bone ($\rho=0.5 \text{ gr/cm}^3$, $E=1\text{MPa}$) which corresponds to the struts of spongy bone at the final healing stages. *In vitro*, we could not follow the five-stage callus simulation of the computational model. Our previous research [15] has shown that a realistic FE modelling of muscle and cartilage would not be properly accomplished as their properties strongly depend on their orientation and on the level of loading when they are compressed by the external fixation within the fracture gap.

Results

We solved the eigenfrequencies problem to identify the normal modes and to compute the resonant frequencies. Fig. 2 shows the bending modes for the intact bone in the case of the free vibrating conditions. One bending mode is identified in the lateral direction with primary resonant frequency at 532Hz (denoted as single bending: SB₁) and a secondary resonance at 985Hz (double bending: DB₁) and a second mode in the anterior-posterior direction with a primary at 546Hz (SB₂) and a secondary at 1064Hz (DB₂). The variation of the resonant frequencies throughout the five maturation stages is plotted in Fig. 2.

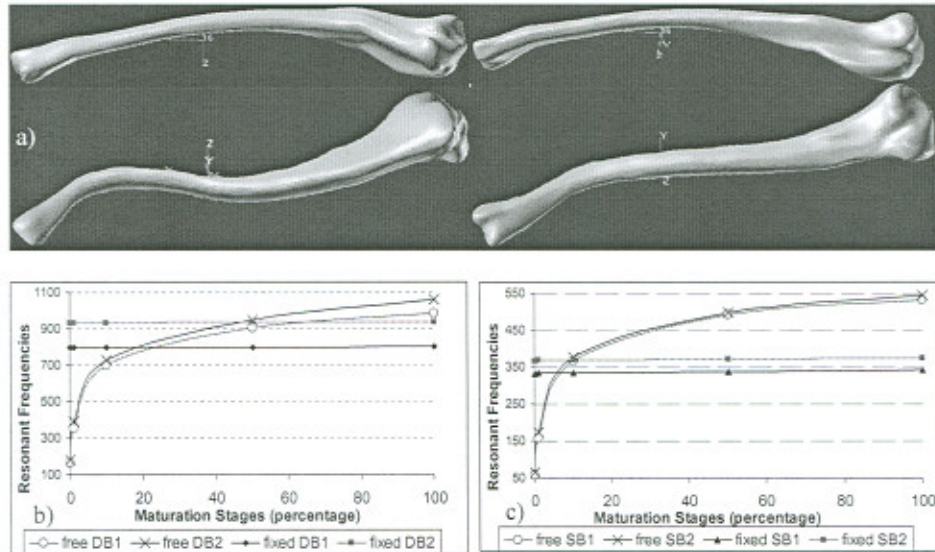


Figure 2: (a) The single and double bending modes in the lateral direction (upper left) and in the anterior-posterior direction (upper right) for the free vibration case. (b), (c): Variation of the resonant frequencies throughout the five maturation stages for the two cases ((b): single bending modes and (c): double bending modes)

Simulation of ultrasound propagation was studied only for the case in which the bone is stabilized by external fixation. The evolution of propagation velocity throughout the five stages is plotted in Fig.3. *In vitro* ultrasound measurements for the three biological materials filling the fracture gap are listed in Table 2. The frequency response (Equation 2) of the FE model calculated at the central frequency of the excitation pulse (1MHz) is shown in Table 3. Furthermore, integration of $A(f)$ over the entire bandwidth yields the attenuation of the excitation pulse as it propagates through the bone at the various maturation stages (Table 3)

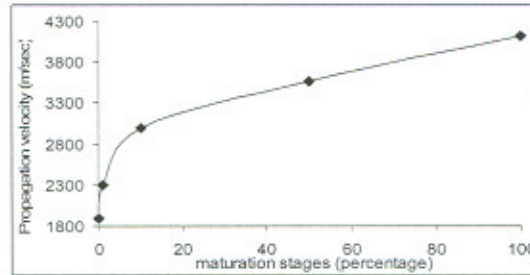


Figure 3: Evolution of ultrasound velocity throughout the five callus maturation stages

Table 2: *In vitro* ultrasound velocity measurements (m/sec)

Simulation material	<i>In vitro</i> velocity
Muscle	2400
Cartilage	3244
Spongy bone	3618
Intact bone	4115

Table 3: Frequency response at 1MHz and wave attenuation within entire bandwidth measurements

Maturation stage	Freq. Resp. $A(f)$ at 1 MHz (dB)	Attenuation (db)
0.1%	40.9	80.2
1%	39.6	78.9
10%	38.6	77.2
50%	34.6	65.1
100%	27.2	50.5

Discussion

Our computed resonant frequencies are in agreement with previous studies [3,5,6]. Furthermore, bending stiffness is lower in the lateral direction (mainly due to smaller cross-sectional area) which results in lower resonant frequencies than in the sagittal plane and this is confirmed by our results. Resonance frequencies are nearly an exponential function of callus material properties for the free vibration case. When bone is fixed at the external fixation, there is a slight increase in resonant frequencies during maturation due to the high damping of the fixation. Ultrasound velocity also exhibits an exponential dependence on callus properties. Frequency response (at 1MHz) and attenuation of the ultrasound wave energy show a linear dependence in decibels (dB), thus an exponential dependence in the linear scale. Lack of similar data in the literature does not allow for comparison of our results. *In vitro*, ultrasound measurements provide with nearly a linear velocity increase for the three materials and the intact bone. The mechanical properties of these materials indicate that Young's modulus has the main contribution to ultrasound velocity.

Acknowledgments

This work is partially funded by the European Union (USBone Project, IST-2000-26350: "A Remotely Monitored Wearable Ultrasound Device for the Monitoring and Acceleration of Bone healing").

References

- 1 Lewis J.L. (1975): "A Dynamic Model of a Healing Fracture Long Bone", *J. Biomech.*, Vol 8, pp 17-25.
- 2 Van der Perre G. (1984): "Dynamic Analysis of Human Bones", *J. Biomech. Eng.*, 11, pp. 87-96.
- 3 Nakatsuchi Y., Tsuchikane A. and Nomura A. (1996): "The Vibrational mode of the Tibia and Assessment of Bone Union in Experimental Fracture Healing Using the impulse Response Method", *Med. Eng. Phys.*, Vol. 18 (7), pp. 575-583.
- 4 Hobatho M, Darmana R., Pastor P., Barrau J.J., Laroze S. and Morucci J.P. (1991): "Development of a Three-Dimensional Finite Element Model of a human tibia Using Experimental modal Analysis", *J. Biomech.*, Vol. 24 (6) pp. 371-383.
- 5 Lowet G., Dayuan X. and Van der Perre G. (1996): "Study of the Vibrational Behaviour of a Healing Tibia Using Finite Element Modelling", *J. Biomech.*, Vol. 29 (8), pp. 1003-1010.
- 6 Couteau B., Hobatho M, Darmana R., Brignola J. and Arlaud J. (1998): "Finite Element Modelling of the Vibrational Behaviour of the Human Femur Using CT-Based Individualized Geometrical and Material Properties", *J. Biomech.*, No 31, pp. 383-386.
- 7 Charalampopoulos A., Fotiadis D.I. and Massalas C.V. (1998): "Free Vibrations of a Double Layered Elastic isotropic Cylindrical Rod", *Int. J. Eng. Sci.*, Vol. 36., pp. 711-731.
- 8 Anast T, Fields T. and Hsueh A. (1958): "Ultrasonic technique for the evaluation of bone fracture", *Am. J. Phys Med.*, 37, pp. 157.
- 9 J. Saulgozis, L. Pontaga and G. Van Der Perre G. (1996): "The effect of fracture and fracture fixation on ultrasonic velocity and attenuation", *Physiol. Meas.*, 17 (3), pp. 201-211.
- 10 Lowet G. and Van Der Perre G. (1996): Ultrasound velocity measurements in long bones: Measurement method and simulation of ultrasound wave propagation. *J. Biomech.*, 29 (10), pp. 1255-1262.
- 11 Njeh C., Hans D., Wu C., Kantorovich E., Sister M., Fuerst T. and Genant H. (1999): "An *in vitro* investigation of the dependence on sample thickness of the speed of sound along the specimen", *Med. Eng. Phys.*, 21, pp. 651-659.
- 12 Malizos K., Hantes M., Mavrodontidis A., Plissiti M., Fotiadis D.I., Massalas C. and Moukarika A. (1999): "Quantitative monitoring and prognosis of osteogenesis", *Med. Biol. Eng. Comp.* 37, Suppl. 2, pp. 288-290.
- 13 Protopappas V., Baga D., Fotiadis D.I., Likas A., Papachristos A. and Malizos K.N. (2002): "An Intelligent Wearable System for the Monitoring of Fracture Healing of Long Bones", *EMBE'02, IFMBE Proc.*, Part2, pp. 978-979.
- 14 Wirtz D.C., Schiffers N., Pandolf T., Radermacher K., Weichert D and Forst R. (2000): "Critical Evaluation of Known Material Properties to Realize Anisotropic FE-simulation of the Proximal Femur", *J. Biomech.*, Vol 33, pp. 1325-1337.
- 15 Kourtis I., Protopappas V., Kourtis L. and Fotiadis D.I. (2002) "A Finite Element Study of Long Bones during Callus Formation". *EMBE'02, IFMBE Proc.*, Part1, pp. 226-227.